Joint Diseases and Related Surgery

Jt Dis Relat Surg
2026;37(1):156-169

ORIGINAL ARTICLE

A comparative analysis of different suture-button orientations for optimal dynamic stabilization of injured syndesmosis: A finite element study

Kazım Taşar, MD[1], Mehmet Kemal Gürsoy, MD[2], Levent Uğur, MD[3], Osman Civan, MD[4], Hakan Özdemir, MD[5]

[1]Department of Orthopedics and Traumatology, Antalya Korkuteli State Hospital, Antalya Türkiye
[2]Department of Orthopedics and Traumatology, Van Training and Research Hospital, Van, Türkiye
[3]Department of Mechanical Engineering, Amasya University, Faculty of Engineering, Amasya, Türkiye
[4]Department of Orthopedics and Traumatology, Private Akdeniz Health Foundation Yaşam Hospital, Antalya, Türkiye
[5]Department of Orthopedics and Traumatology, Akdeniz University Faculty of Medicine, Antalya, Türkiye

The tibiofibular syndesmosis is a fibrous joint in which the tibia and fibula are connected by a strong membrane and ligamentous structures.[1] This complex anatomical configuration includes the anteroinferior tibiofibular ligament (AITFL), posteroinferior tibiofibular ligament (PITFL), interosseous ligament (IOL), and transverse tibiofibular ligament (TTFL). It possesses sufficient flexibility to permit small-scale rotational and translational movements of the fibula during different phases of gait.[2] Syndesmotic injuries typically occur following high-energy trauma,

Received: March 11, 2025
Accepted: August 05, 2025
Published online: October 08, 2025

Correspondence: Mehmet Kemal Gürsoy, MD. Van Eğitim ve Araştırma Hastanesi, Ortopedi ve Travmatoloji Kliniği, 65300 Edremit, Van Türkiye.

E-mail: mehmetkemalgursoy07@gmail.com

Doi: 10.52312/jdrs.2026.2258

Citation: Taşar K, Gürsoy MK, Uğur L, Civan O, Özdemir H. A comparative analysis of different suture-button orientations for optimal dynamic stabilization of injured syndesmosis: A finite element study. Jt Dis Relat Surg 2026;37(1):156-169. Doi: 10.52312/jdrs.2026.2258

ABSTRACT

Objectives: This study aims to identify the optimal suture-button orientation which supports physiological ligament healing by limiting pathological lateral and posterior translation, as well as rotational motion in the axial plane of the syndesmosis joint, through dynamic suture-button fixation.

Materials and methods: A solid ankle model and a syndesmotic injury model were developed using finite element analysis. To address the syndesmotic injury, five different suture-button fixation configurations were designed. These models were analyzed by simulating the loading conditions during the heel-off phase of the stance phase. Evaluations included fibular displacement in the anterior-posterior and medial-lateral planes, rotational angles in the axial plane, and measurements of anterior and posterior tibiofibular clear space (A-TFCS and P-TFCS).

Results: All models utilizing double suture-buttons demonstrated superior control of pathological fibular motion compared to the conventional single suture-button fixation technique (Model 1). Among them, the configuration employing double suture-buttons aligned with the anatomical orientations of the AITFL and PITFL (Model 3) was the most effective in achieving anatomical reduction and preserving physiological fibular motion. Model 5, which was specifically designed to minimize the risk of injury to neurovascular structures, tendons, and articular cartilage, reduced pathological displacement in the coronal and sagittal planes by 3% and 1%, respectively, compared to Model 3. However, it exhibited a 0.5° deficiency in limiting external rotation relative to Model 3.

Conclusion: The results obtained with Model 5 closely approximate those of the healthy ankle and demonstrate its potential as a promising fixation method which preserves critical anatomical structures. This model allows for anatomical reduction of the syndesmosis, effectively prevents pathological syndesmotic motion, and maintains physiological fibular movement. In light of these findings, we believe that Model 5 may be among the preferred techniques in the treatment strategies for syndesmotic injuries.

Keywords: Finite element, suture-button, syndesmotic injury, tibiofibular joint.

athletic activities, or torsional stress to the ankle. If not appropriately managed, such injuries may result in long-term complications including chronic instability, post-traumatic arthrosis, and functional impairment.[3]

Regarding the performance of suture-button systems and conventional screw fixation methods for the treatment of syndesmotic injuries, it has been reported that conventional screw fixation limits physiological fibular motion due to its rigid structure leading to complications such as screw loosening or breakage.[4-7] In contrast, suture-button fixation is associated with lower complication rates compared to conventional screw fixation techniques.[8-11] Additionally, suture-button systems have been shown to significantly reduce the risk of malreduction, provide biomechanical strength comparable to traditional methods, allow greater postoperative range of motion, and promote ligament healing by enabling a more flexible form of stabilization that supports natural recovery processes.[8-11]

There is also evidence indicating that syndesmotic widening in the loaded ankle following suture-button fixation is comparable to that observed in an intact, healthy ankle.[8-11] However, there is still no consensus regarding the ability of suture-button constructs to adequately restrict fibular external rotation and posterior translation.[1,12-14] Although various suture-button configurations have been proposed for the treatment of syndesmotic injuries, the optimal method/configuration for such injuries remains unclear.[2]

Comprehensive studies evaluating the biomechanical effects of suture-button techniques applied in various configurations for the treatment of syndesmotic injuries on the distal tibiofibular joint remain limited. In the present study, we aimed to assess parameters related to distal tibiofibular joint stability by employing finite element analysis (FEA) and to evaluate different suture-button configurations in a model of unstable syndesmotic injury.

MATERIALS AND METHODS

In our study, following the three-dimensional (3D) modeling of a healthy ankle using computed tomography (CT) images, a model simulating syndesmotic injury was developed. Subsequently, five different fixation configurations employing a flexible fixation method suture-button were evaluated to determine the extent to which supraphysiological anterior-posterior and medial-lateral translations of the fibula in the sagittal plane, as well as rotational movement in the axial plane, could be limited in unstable syndesmotic injuries. For this purpose, biomechanical analyses were conducted using FEA to assess the distal tibiofibular clear space distance, the degree of external fibular rotation, and the amount of fibular translation along the x-, y-, and z-axes.

Preparation of 3D model

The right lower extremity of a healthy adult male individual, 35 years old, weighing 70 kg and 170 cm tall, was scanned with CT at 0.5-mm slice intervals from the sole to the level of the knee joint. The device employed during the scan obtained images at a resolution of 512×512 pixels with a pixel size of 0.75 mm at an energy level of 120 kV. A total of 1000 slices were taken, and these slices were stored in Digital Imaging and Communications in Medicine (DiCOM) format. There was no history of trauma in the patient's history. Also, no pathology was detected in the physical examination and imaging. The DICOM data were analyzed using the 3D modeling software MIMICS® 12.11 (Materialise, Leuven, Belgium). Bone structures (tibia, fibula, talus, calcaneus, and navicular) were converted to stereolithography (STL) format by correcting the surface geometry and removing artifacts. The data in STL format was, then, transferred to the reverse engineering software GEOMAGIC® Studio (Geomagic, Durham, NC, USA) to edit the surface roughness and complete the missing parts. In this context, Non-Uniform Rational B-Splines (NURBS) surfaces were created and the final model was created using SolidWorks® (Dassault Systèmes, Waltham, MA, USA) software. Cancellous and cortical bone structures were defined in SolidWorks software and a model which was suitable for FEA was created.

Modeling of the ligaments

The anatomical structures of the ligaments which play roles in stabilizing the lower extremity were modeled based on literature data. In this context, AITFL, PITFL, transverse A total of 19 ligaments, including the TTFL, IOL, and deltoid ligament, were designed as 3D solid models by taking into account their anatomical attachment points and their lengths in the neutral position (Figure 1). During the modeling process, the distances between the attachment points of the ligaments were defined following the values specified in the literature.[15-19]

FIGURE 1. Lower extremity ligaments, interosseous membrane and finite element model mesh structure.

Finite element model and material characteristics

The model which was prepared for FEA was prepared using ANSYS Workbench version 19.0 (Ansys Inc., Canonsburg, PA, USA) software. In creating the mesh structure, the mesh size was determined as 5 mm for bone structures and 1 mm for ligaments. The resulting model consists of approximately 685962 nodes and 452828 elements. Cortical bone, cancellous bone, suture-button systems, and ligaments were defined according to the isotropic material characteristics specified in the literature.[20-22] The elastic modulus and Poisson's ratio values for cortical bone and cancellous bone are shown in Table I, and the mechanical characteristics of the ligaments are shown in Table II. A "frictionless" contact condition was defined between the bone structures and the interaction between the suture button and the cortical and cancellous bone was modeled in the same way. Seven different models were prepared for loading scenarios after the material and contact definitions were completed.

Injury model and fixation techniques

Syndesmosis injuries are classified in different ways depending on factors such as the force intensity, direction, and position of the foot at the time of the trauma. The present study was based on the Sikka classification employed for isolated syndesmosis injuries. Although Stage 1 injuries are managed with conservative treatment, surgical fixation is recommended for unstable injuries such as Stage 3 and Stage 4.[23] Our model was conducted by removing the AITFL, PITFL, TTFL,

TABLE I
Bone and suture-button material characteristics

Materials	Young's modulus (E), MPa	Poisson's ratio (ν)
Cortical bone	17000	0.3
Cancellous bone	700	0.2
No. 5 FiberWire	380000	0.39
Suture-button titanium	96000	0.36

TABLE II
Mechanical characteristics of ligaments

Ligament	Young's modulus (E), MPa	Poisson's ratio (ν)
Anteroinferior tibiofibular ligament	160	0.49
Posteroinferior tibiofibular ligament	160	0.49
Transverse tibiofibular ligament	160	0.49
Interosseous ligament	260	0.4
Anterior talofibular ligament	255.5	0.49
Posterior talofibular ligament	216.5	0.49
Calcaneofibular ligament	512	0.49
Interosseous talocalcaneal ligament	260	0.4
Cervical ligament	260	0.4
Lateral talocalcaneal ligament	260	0.4
Posterior talocalcaneal ligament	260	0.4
Medial talocalcaneal ligament	260	0.4
Talonavicular ligament	260	0.4
Deep anterior tibiotalar ligament	184.5	0.49
Deep posterior tibiotalar ligament	99.5	0.49
Tibiocalcaneal ligament	512	0.49
Tibionavicular ligament	512	0.49
Superficial posterior tibiotalar ligament	512	0.49
Tibiospring ligament	512	0.49
Interosseous membrane	260	0.4

IOL, and the deltoid ligament complex to simulate a Sikka Stage 4 isolated syndesmotic injury.[24] In the present study, five different suture-button fixation models were developed for the treatment of inferior tibiofibular syndesmosis injuries. The first model, conventional fixation (Model 1), was created by placing the suture button parallel to the tibiotalar joint in the coronal plane and at a 30° anteromedial angle in the transverse plane, 1.5 cm proximal to the plafond. Divergence fixation (Model 2) the first suture-button was applied 1.5 cm proximal to the plafond, in the coronal plane parallel to the tibiotalar joint, and in the transverse plane at a 45° anteromedial orientation. The second suture-button was placed 1 cm proximal to the first one, with a 30° anteromedial orientation. The third model, fixation appropriate to AITFL and PITFL axis (Model 3). In this model, which aimed to mimic the AITFL, extending at an angle of 30 to 50° in the coronal plane and 65° in the sagittal plane relative to the tibial plafond, and the PITFL, extending at an angle of 20 to 40° in the coronal plane and 60 to 85° in the sagittal plane; the first suture-button, simulating the AITFL, was placed at the joint level through the distal posterior edge of the fibula, with a 45° anteromedial orientation in the coronal plane and 65° in the transverse plane; the second suture-button, simulating the PITFL, was inserted at the joint level through the anterior edge of the fibula, with a 30° posteromedial orientation in the coronal plane and 60° in the transverse plane, vascular, nerve and tendon sparing fixation (Model 4). In the third model, without altering the entry points of the suture-buttons at the joint level, the first suture-button was applied with a 45° anteromedial orientation in the coronal plane relative to the plafond, and in the transverse plane, based on the anteromedial corner of the tibial crest; the second suture-button was applied with a 30° orientation in the coronal plane relative to the plafond, and with a 20° posteromedial orientation in the transverse plane, based on the posteromedial corner of the tibial crest. Finally, vascular, nerve, tendon and cartilage-sparing fixation (Model 5) to avoid iatrogenic cartilage damage in the tibiofibular cartilage contact zone (TFCCZ), the suture-buttons in Model 4 were applied with the same orientations, but with entry points located 1 cm proximal to the joint level on the fibula. All fixation models are shown in Figure 2. These models were, then,

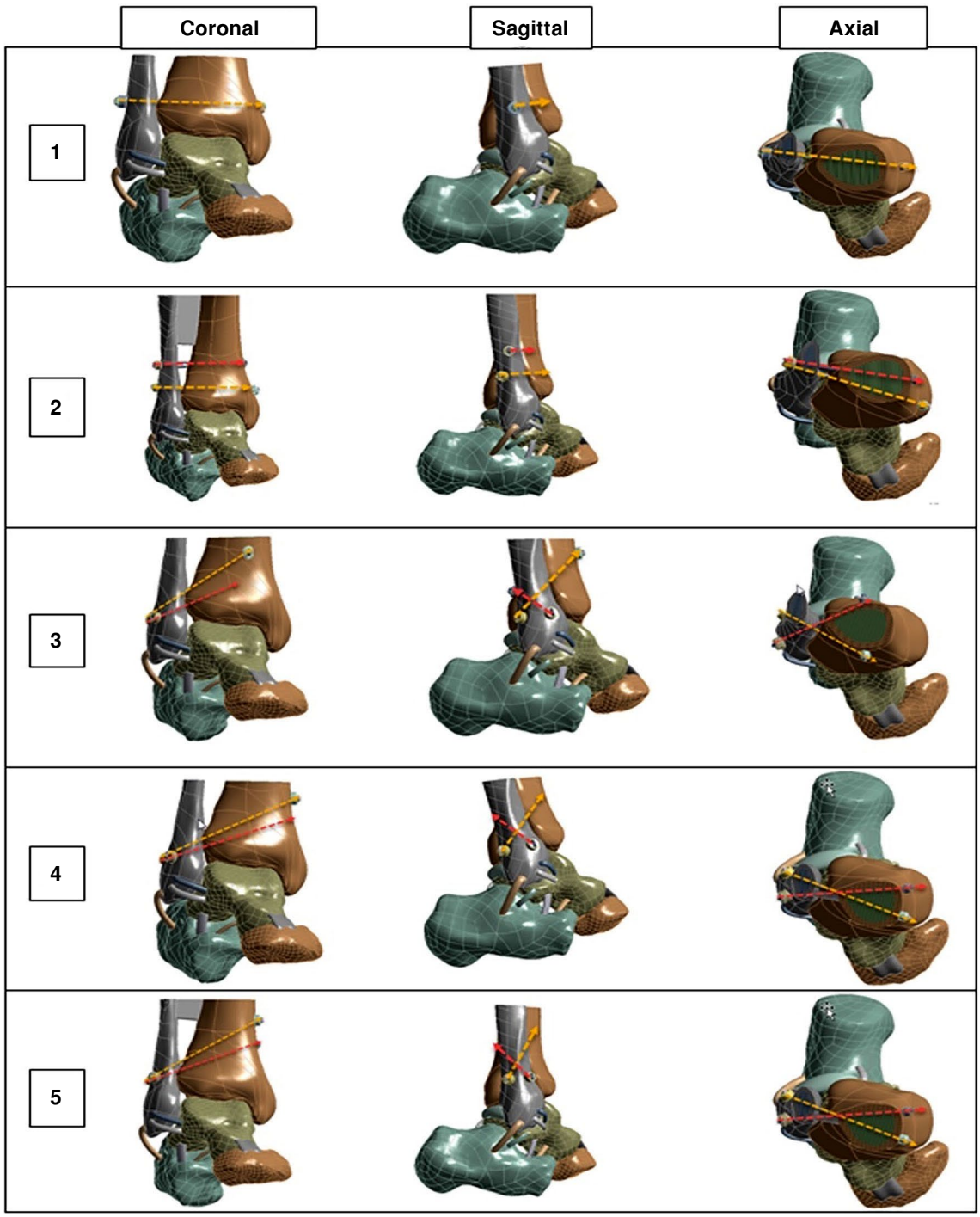

FIGURE 2. Syndesmosis injury model and fixation modalities.

evaluated in line with different biomechanical requirements and clinical scenarios.[25]

Loading and simulation

During ankle dorsiflexion, the distal fibula moves slightly away from the tibia, allowing expansion of the ankle mortise. This dynamic separation is facilitated by the syndesmotic ligaments, which connect the distal ends of the tibia and fibula and possess physiological elasticity. To better understand the physiological behavior of the syndesmosis, the "heel-off" phase corresponding to the fourth sub-phase of the stance phase in the gait cycle was simulated. In the modeling, while the ankle was

dorsiflexed by 10°, a compressive force of 3528 N and an anteriorly directed tangential force of 533 N were applied to the tibial plateau, followed by sagittal, coronal, rotational movements of the fibula and tibial fibular clear space measurements were made (Figure 3). In the present model, only the forces of the Achilles and tibialis anterior tendons were considered; other tendon forces and mediolateral forces were not included in the analysis.[26,27]

Defining the anatomical coordinate system

An anatomical coordinate system was established to facilitate the interpretation of post-loading translations. The x-axis was aligned parallel to the anatomical axis of the tibia. The y-axis was defined as the line connecting the long axis of the calcaneus to the midpoint of the second metatarsal head. The z-axis was designated as the line extending medially from the tip of the lateral malleolus toward the opposite malleolus (Figure 4).

Statistical analysis

Statistical analysis was performed using the GraphPad Prism version 9.0 (GraphPad Software, San Diego, CA, USA). Continuous data were expressed in mean ± standard deviation (SD) or median (min-max), categorical data were expressed in number and frequency. The distribution of the data was assessed using the Shapiro-Wilk test. Comparisons among the intact ankle, the injury model, and the five fixation configurations were performed using one-way analysis of variance (ANOVA), and Tukey's post-hoc test was applied for multiple comparisons. A p value of <005 was considered statistically significant.

RESULTS

The biomechanical performance of suture-button fixation techniques was analyzed in the present study. Consistent with previous biomechanical investigations, the outcomes included lateral translation of the fibula relative to the tibia, posterior translation, external rotation relative to the tibia, and tibiofibular distance measurements.[14,24]

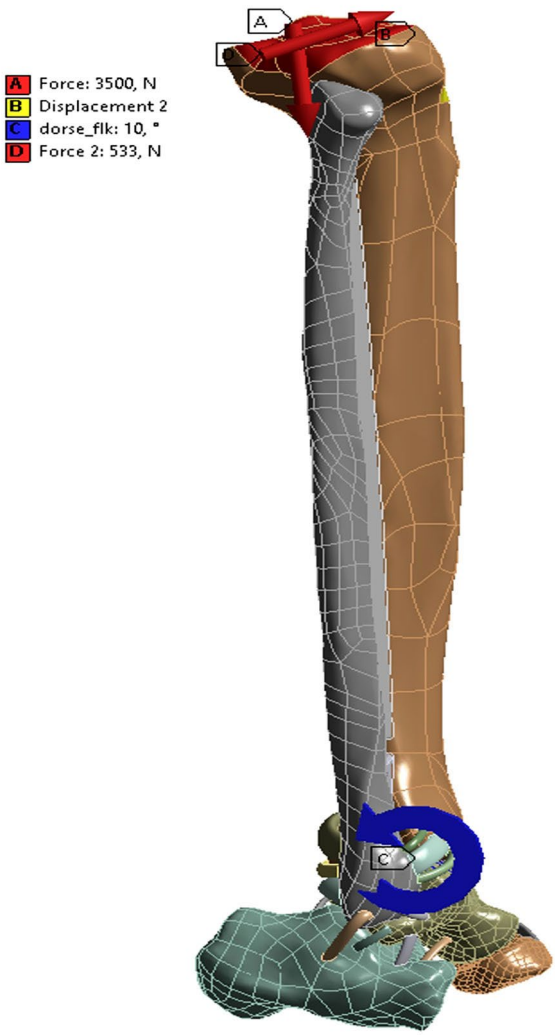

FIGURE 3. Loading model and applied forces.

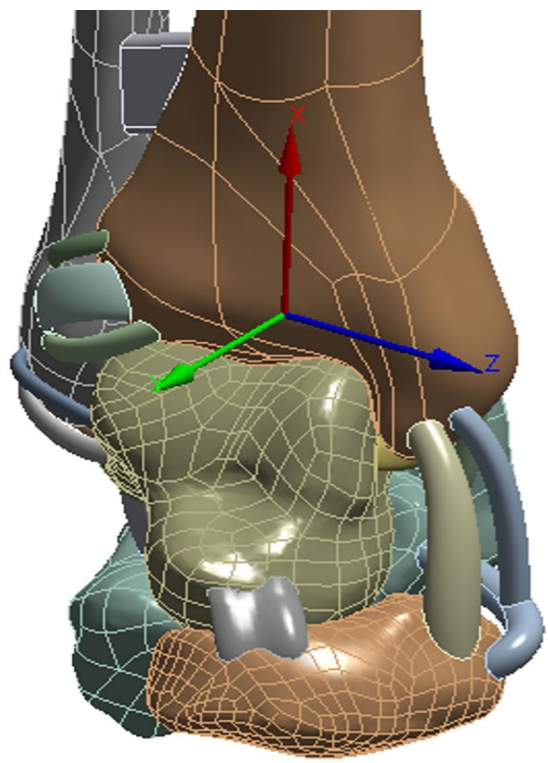

FIGURE 4. Definition of the anatomical coordinate system.

In addition to previous studies, our simulations also include measurements of the anterior and posterior tibiofibular clear space.

In the injury model, external rotation increased significantly compared with the intact ankle (13.840° *vs.* 1.170°, p<0.001). Conventional single suture-button fixation (Model 1: 4.950°) partially reduced this displacement but did not achieve physiological values (p<0.01). In contrast, the anatomical configuration replicating the AITFL and PITFL axes (Model 3: 1.6905°) and the neurovascular- and cartilage-sparing fixation (Model 5: 2.224°) produced values closest to the intact model, with no statistically significant difference (p>0.05). Tibiofibular clear space measurements revealed anterior widening (A-TFCS: 4.757 mm) and posterior narrowing (P-TFCS: 1.713 mm) in the injury model compared with the intact loaded ankle (A-TFCS: 2.243 mm, P-TFCS: 5.098 mm) (p<0.001). Model 3 (A-TFCS: 2.284 mm, P-TFCS: 4.661 mm) and Model 5 (A-TFCS: 2.296 mm, P-TFCS: 4.343 mm) provided values closest to those of the intact ankle (p>0.05). Similarly, supraphysiological posterior (–2.682 mm) and lateral (–3.123 mm) displacements observed in the injury model were only partially corrected by Model 1 (AP: 0.098 mm, ML: –1.007 mm), whereas near-physiological values were obtained with Model 3 (AP: 0.566 mm, ML: –0.544 mm) and Model 5 (AP: 0.532 mm, ML: –0.613 mm). These findings indicate that multi–suture-button configurations aligned with anatomical orientations provide more effective restoration of physiological fibular motion compared with conventional fixation.

Displacement of the fibula in the anteroposterior plane according to the anatomical coordinate system

In the loading condition based on the forces effective in the fourth stage of the stance stage of walking, an anterior displacement of 0.755 mm was detected in the fibula in the model representing the healthy ankle. In the Sikka Stage 4, isolated syndesmotic injury model created by removing the ligaments representing the AITFL, PITFL, TTFL, and IOL, a posterior translation of 2.682 mm appeared. Although the supraphysiological displacement of the fibula in the posterior direction in the sagittal plane could be limited by 80% in the traditional fixation method, Model 1, physiological values could not be obtained. Compared to the healthy ankle model, the supraphysiological posterior translation appearing in the anteroposterior plane was limited by 94.5%, 94.6%, and 93.5% in Models 3, 4, and 5, respectively, and the closest values to the healthy ankle were obtained (Figure 5).

Displacement of the fibula in the mediolateral plane according to the anatomical coordinate system

When the loading model was applied, 0.278 mm lateral displacement appeared in the fibula in the intact ankle model, but after the syndesmotic ligaments were injured, the lateral translation increased significantly to 3.123 mm. Although 74% of the supraphysiological movement could be limited in the traditional fixation method

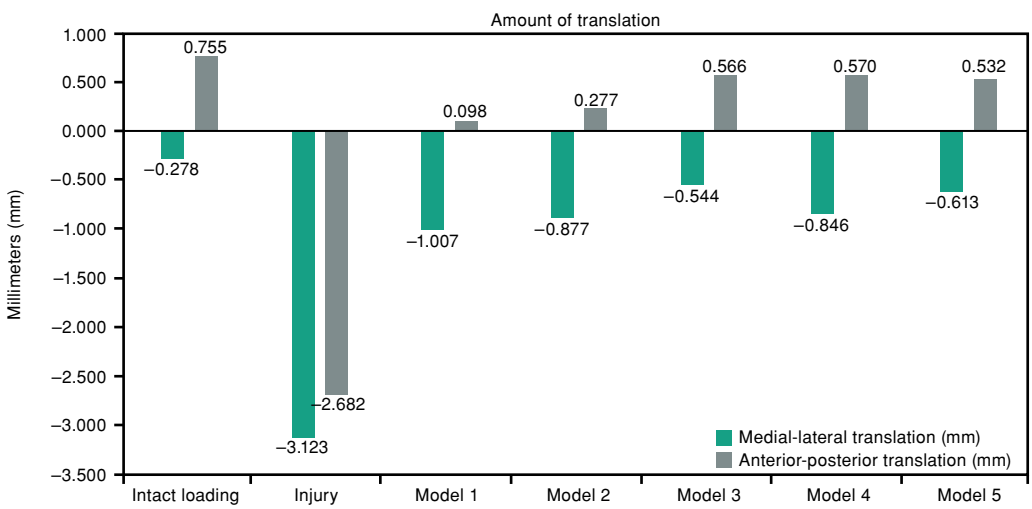

FIGURE 5. Anterior-posterior translation: (+) anterior, (–) posterior; medial-lateral translation of the fibula: (+) medial, (–) lateral.

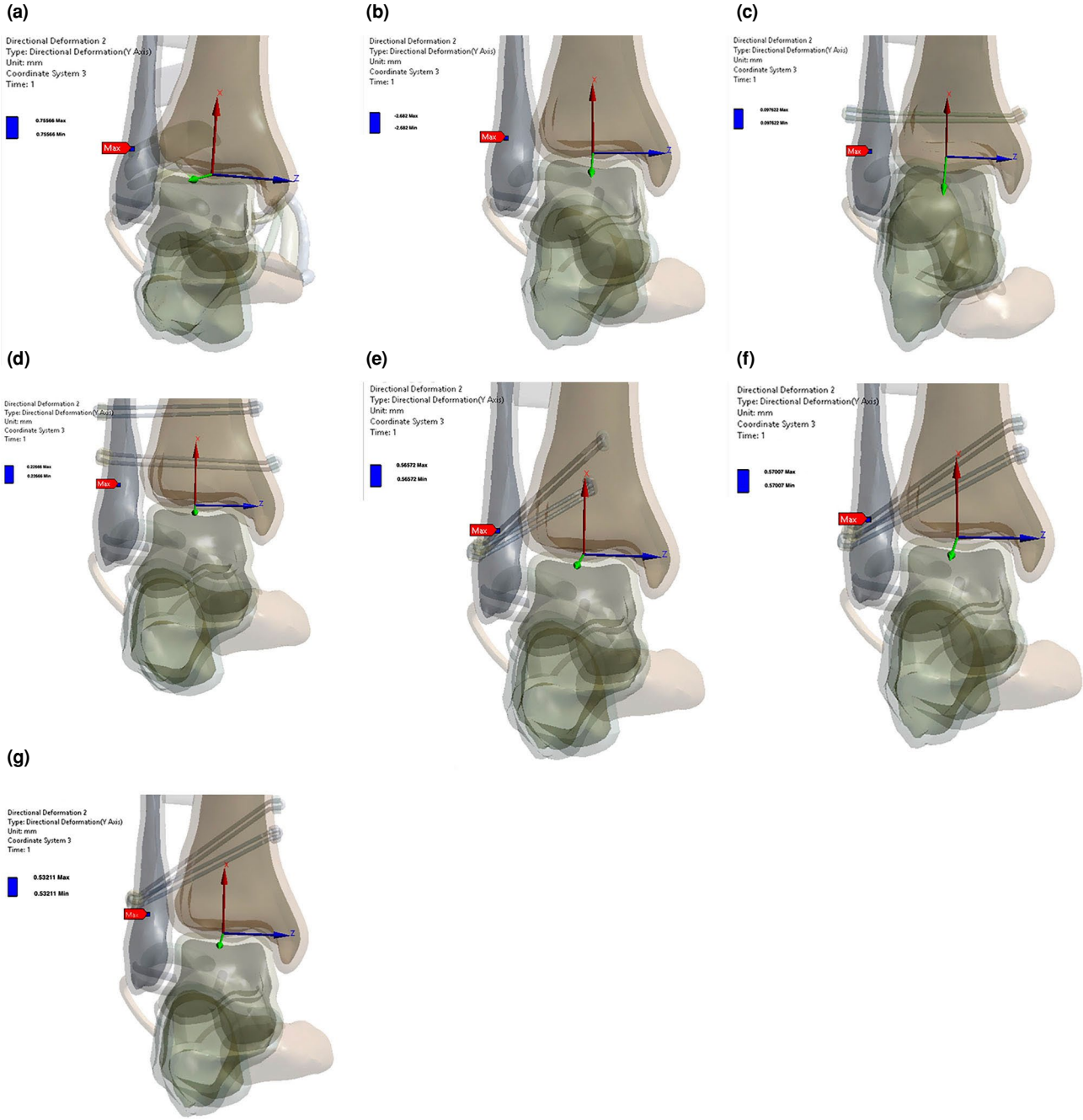

FIGURE 6. Anterior-posterior translation of the fibula following loading. **(a)** intact syndesmosis model, **(b)** syndesmosis injury model, **(c)** conventional fixation (Model 1), **(d)** divergence fixation (Model 2), **(e)** fixation appropriate to AITFL and PITFL axis (Model 3), **(f)** vascular, nerve and tendon sparing fixation (Model 4), **(g)** vascular, nerve, tendon and cartilage-sparing fixation (Model 5).
AITFL: Anteroinferior tibiofibular ligament; PITFL: Posteroinferior tibiofibular ligament.

(Model 1), 91% and 88% of the supraphysiological movement were limited in Model 3 and Model 5, respectively, and values closer to physiological translation were obtained (Figure 5). The translation of the fibula in the anteroposterior plane and medial-lateral plane obtained as a result of the analyses is given in Figure 6 and 7.

Rotational displacement of the fibula

During the loading, 1.170° external rotation developed in the healthy ankle, while the rotation increased to 13.840° in the case of syndesmotic injury. Although the external rotation of the fibula might be limited up to 4.950° in Model 1, which is

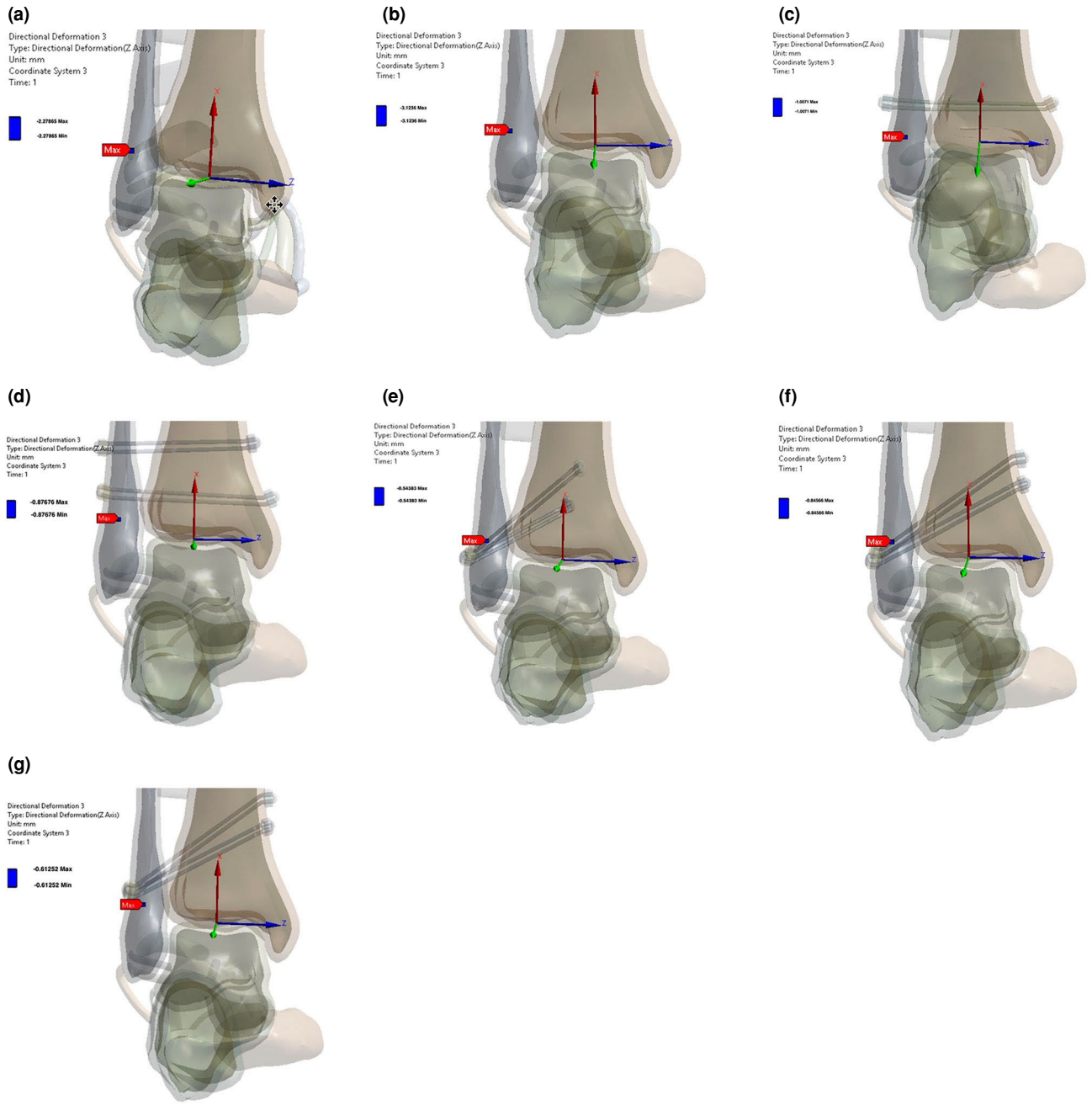

FIGURE 7. Medial-lateral translation of the fibula following loading. **(a)** intact syndesmosis model, **(b)** syndesmosis injury model, **(c)** conventional fixation (Model 1), **(d)** divergence fixation (Model 2), **(e)** fixation appropriate to AITFL and PITFL axis (Model 3), **(f)** vascular, nerve and tendon sparing fixation (Model 4), **(g)** vascular, nerve, tendon and cartilage-sparing fixation (Model 5).
AITFL: Anteroinferior tibiofibular ligament; PITFL: Posteroinferior tibiofibular ligament.

the traditional fixation method, 1.6905° rotation was provided in Model 3, mimicking the ITFL and PITFL orientation, and the closest values to the healthy model were obtained. In Model 5, which we designed with the idea that it would minimize complications in clinical practice, although the rotation might be limited up to 2.224°, more favorable results were obtained than the traditional fixation method, and values close to physiological rotation were obtained (Figure 8).

Tibiofibular clear space

The distance between the anterior tibial tubercle and the lateral edge of the fibula

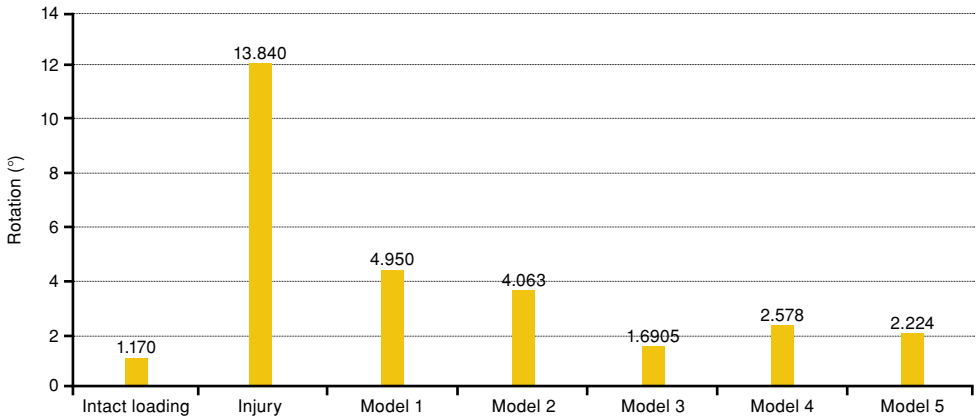

FIGURE 8. Rotation of the fibula during loading in dorsiflexion.

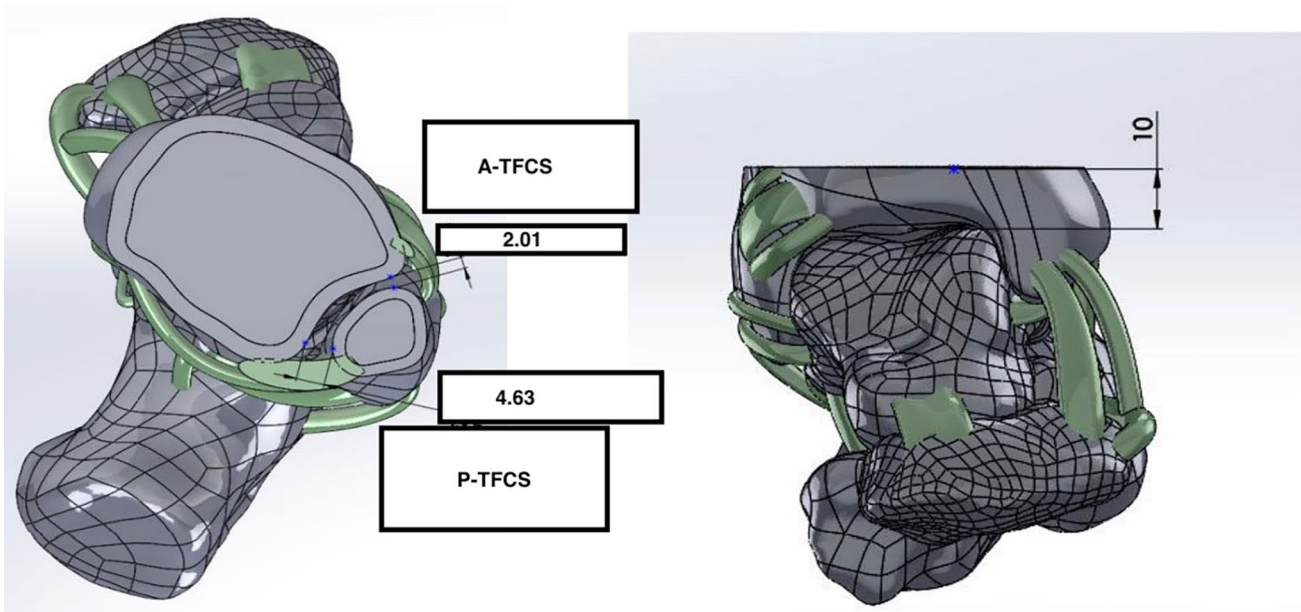

FIGURE 9. Measurements of anterior (A-TFCS) and posterior (P-TFCS) tibiofibular clear space.
A-TFCS: Anterior tibiofibular clear space; P-TFCS: Posterior tibiofibular clear space.

(anterior tibiofibular clear space [A-TFCS]) and the distance between the posterior tibial tubercle and the lateral edge of the fibula (posterior tibiofibular clear space [P-TFCS]) were measured and recorded in all models, 1 cm proximal to the ankle joint level (Figures 9 and 10). Although the A-TFCS and P-TFCS values in the unloaded healthy ankle were measured at 2.010 mm and 4.630 mm, respectively, both distances increased following loading in the dorsiflexion position, reaching 2.243 mm and 5.098 mm. In contrast to the healthy model, in the syndesmotic injury model under loading, an increase in A-TFCS and a decrease in P-TFCS were observed. Among the fixation models, Model 3 produced values closest to those of the loaded healthy ankle.

DISCUSSION

In the present study, we assessed parameters related to distal tibiofibular joint stability by employing FEA and evaluated different suture-button configurations in a model of unstable syndesmotic injury. The most physiological replication of fibular motion and anatomical syndesmosis reduction was achieved with the dynamic syndesmosis fixation method described

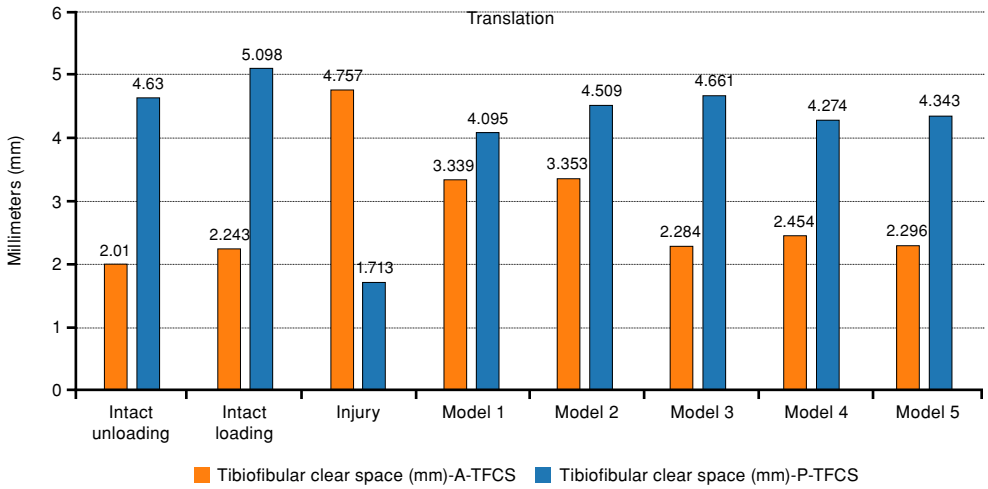

FIGURE 10. Anterior (A-TFCS) and posterior (P-TFCS) tibiofibular clear space values.

in Model 3, which was based on replicating the anatomical orientations of the AITFL and PITFLs. Model 5, which was developed to reduce the risk of injury to vascular, neural, cartilaginous, and tendinous structures, demonstrated the second-best performance among the dynamic fixation configurations, following Model 3.

Conventional suture-button fixation (Model 1) has been shown to limit supraphysiological lateral translation of the fibula and reduce posterior translation by approximately 80%. Despite these effects, the technique remains inadequate in restoring physiological fibular motion. These findings align with previous research indicating that suture-button systems have limited capacity to control fibular movement in the sagittal plane.[6,28-30] Therefore, achieving physiological syndesmotic fixation appears unattainable with this method alone. While some studies have suggested that single suture-button constructs provide biomechanical performance similar to that of a healthy ankle,[14,31] the present results and existing literature collectively imply that conventional suture-button systems are unlikely to offer optimal treatment for unstable syndesmotic injuries.

Models utilizing two suture-buttons in various configurations demonstrated biomechanical behavior more closely aligned with the physiological properties of the native ankle than the conventional single suture-button fixation (Model 1). The current body of literature on the biomechanical and functional outcomes of suture-button fixation is predominantly based on single suture-button applications.[8-10] Furthermore, it is well established that anatomical reconstruction after syndesmotic injuries leads to favorable results.[32] In this context, implementing multiple suture-buttons in anatomically aligned configurations appears to offer improved restoration of physiological fibular motion. The biomechanical data presented herein support this approach. Nonetheless, it should be acknowledged that conflicting results have been reported in previous studies.[33,34] A key factor contributing to these inconsistencies may be the limited scope of earlier investigations, which often focused solely on parallel or divergent two-suture-button configurations, without incorporating anatomically accurate orientations such as those mimicking the AITFL and PITFL.[13,24,33] Notably, O'Daly et al.[34] observed outcomes closely approximating those of the healthy ankle when adopting anatomical alignments based on AITFL and PITFL orientations. Consistent with these findings, fixation models emulating the anatomical axes of the AITFL and PITFL (Model 3), neurovascular- and tendon-sparing fixation (Model 4), and configurations designed to protect vascular, neural, cartilaginous, and tendinous structures (Model 5) also yielded similar results.

Beyond the existing literature, the fixation techniques detailed in the models particularly the configuration replicating the anatomical axes of the AITFL and PITFL (Model 3), and the approach designed to preserve vascular, neural, joint cartilage, and tendinous structures (Model 5) achieved fibular lateral, posterior, and external rotation values closely approximating those of the healthy ankle. This outcome is primarily attributed to

the more anatomically accurate alignment of the proposed fixation methods with the orientations of the AITFL and PITFL. The findings are in agreement with previously reported outcomes from anatomical fixation techniques described in earlier studies.[30,32,34,35] Nevertheless, further biomechanical investigations are required to evaluate suture-button fixation under physiological loading conditions using direct anatomical references to the AITFL and PITFL, and to comprehensively assess the post-fixation kinematics of fibular motion under load.

The vascular, nerve, articular cartilage, and tendon sparing fixation technique (Model 5) produced results closely approximating the physiological loading characteristics of the fibula. This model was specifically designed to address the potential risk of neurovascular and other anatomical structure injuries associated with the fixation method (Model 3) which mimics the anatomical axes of the AITFL and PITFL.[9,25] To minimize such risks, we hypothesized that the Model 5 configuration could better preserve neurovascular structures and adjacent tissues.[36] The outcomes supported this hypothesis, demonstrating substantial control over fibular rotation and translation. Consequently, this technique is believed to offer a lower complication profile compared to conventional fixation approaches.

Among the tested models, the vascular, nerve, joint cartilage, and tendon-preserving fixation technique (Model 5) and the fixation configuration replicating the anatomical axes of the AITFL and PITFL (Model 3) demonstrated the closest approximation to the A-TFCS and P-TFCS values of the intact ankle under dynamic loading. Tibiofibular clear space is a critical parameter for evaluating syndesmotic injuries,[37-40] and restoring it to near-physiological levels has been strongly associated with favorable postoperative clinical and radiological outcomes.[41,42] These results indicate that the use of these two fixation models may offer the most effective restoration of physiological syndesmotic integrity.

The results obtained using the conventional fixation method were consistent with previously published data, thereby supporting the validity of the FEA. Nonetheless, several limitations should be acknowledged. The model was created as a homogeneous solid based on computed tomography images from a single individual, and the material properties of bone and ligament structures were derived from earlier studies. Regarding loading conditions, only the fourth phase of the gait stance cycle was simulated; a dynamic representation of the entire cycle was not performed. Moreover, the fixation techniques assessed reflect time-zero mechanical conditions, meaning that aspects such as hardware loosening, suture material creep, and the stabilizing role of surrounding soft tissues were not incorporated. These are intrinsic limitations of finite element analyses and, in this context, are not considered to undermine the study's conclusions. An additional limitation is the omission of tibiotalar contact pressure, which has been highlighted as an important parameter in the evaluation of syndesmotic injuries.[43,44] While the present findings are promising, they should be validated in future experimental and clinical research.

In conclusion, this study demonstrated that double suture-button fixation provides superior control of pathological fibular motion compared with the conventional single suture-button technique. Among the tested configurations, Model 5, a vascular-, nerve-, tendon-, and cartilage-preserving approach, most closely reproduced the biomechanics of a healthy ankle. While it showed a minor limitation in controlling external rotation compared with Model 3, it offered additional advantages in reducing the risk of iatrogenic injury to critical anatomical structures. Taken together, these findings suggest that Model 5 achieves a balance between biomechanical stability and anatomical safety, thereby supporting physiological fibular motion and effective syndesmotic reduction. As such, Model 5 may represent a promising fixation strategy for the management of syndesmotic injuries, warranting further investigation in clinical settings to validate its long-term outcomes and potential role in treatment algorithms.

Data Sharing Statement: The data that support the findings of this study are available from the corresponding author upon reasonable request.

Author Contributions: Obtained data and wrote the paper: M.K.G., K.T., L.U., O.C., H.Ö.

Conflict of Interest: The authors declared no conflicts of interest with respect to the authorship and/or publication of this article.

Funding: The authors received no financial support for the research and/or authorship of this article.

REFERENCES

1. Canton SP, Gale T, Onyeukwu C, Hogan MV, Anderst W. Syndesmosis repair affects in vivo distal interosseous tibiofibular ligament elongation under static loads and during dynamic activities. J Bone Joint Surg Am 2021;103:1927-36. doi: 10.2106/JBJS.20.01787.

2. Vohra R, Singh A, Thorat B, Patel D. Instability of the distal tibiofibular syndesmosis. J Orthop Surg (Hong Kong) 2023;31:10225536231182349. doi: 10.1177/10225536231182349.
3. Elabd A, Abdullah S, Kandel W, Hegazy M. Syndesmotic stabilization: Syndesmotic screw versus flexible fixation: A systematic review. J Foot Ankle Surg 2021;60:998-1007. doi: 10.1053/j.jfas.2020.09.021.
4. den Daas A, van Zuuren WJ, Pelet S, van Noort A, van den Bekerom MP. Flexible stabilization of the distal tibiofibular syndesmosis: Clinical and biomechanical considerations: A review of the literature. Strategies Trauma Limb Reconstr 2012;7:123-9. doi: 10.1007/s11751-012-0147-2.
5. Thornes B, Walsh A, Hislop M, Murray P, O'Brien M. Suture-endobutton fixation of ankle tibio-fibular diastasis: A cadaver study. Foot Ankle Int 2003;24:142-6. doi: 10.1177/107110070302400208.
6. Klitzman R, Zhao H, Zhang LQ, Strohmeyer G, Vora A. Suture-button versus screw fixation of the syndesmosis: A biomechanical analysis. Foot Ankle Int 2010;31:69-75. doi: 10.3113/FAI.2010.0069.
7. LaMothe JM, Baxter JR, Murphy C, Gilbert S, DeSandis B, Drakos MC. Three-dimensional analysis of fibular motion after fixation of syndesmotic ınjuries with a screw or suture-button construct. Foot Ankle Int 2016;37:1350-6. doi: 10.1177/1071100716666865.
8. Xu K, Zhang J, Zhang P, Liang Y, Hu JL, Wang X, et al. Comparison of suture-button versus syndesmotic screw in the treatment of distal tibiofibular syndesmosis injury: A meta-analysis. J Foot Ankle Surg 2021;60:555-66. doi: 10.1053/j.jfas.2020.08.005.
9. Lee JS, Curnutte B, Pan K, Liu J, Ebraheim NA. Biomechanical comparison of suture-button, bioabsorbable screw, and metal screw for ankle syndesmotic repair: A meta-analysis. Foot Ankle Surg 2021;27:117-22. doi: 10.1016/j.fas.2020.03.008.
10. Migliorini F, Maffulli N, Cocconi F, Schäfer L, Bell A, Katusic D, et al. Better outcomes using suture button compared to screw fixation in talofibular syndesmotic injuries of the ankle: A level I evidence-based meta-analysis. Arch Orthop Trauma Surg 2024;144:2641-53. doi: 10.1007/s00402-024-05354-x.
11. Andersen MR, Frihagen F, Hellund JC, Madsen JE, Figved W. Randomized trial comparing suture button with single syndesmotic screw for syndesmosis injury. J Bone Joint Surg Am 2018;100:2-12. doi: 10.2106/JBJS.16.01011.
12. Clanton TO, Whitlow SR, Williams BT, Liechti DJ, Backus JD, Dornan GJ, et al. Biomechanical comparison of 3 current ankle syndesmosis repair techniques. Foot Ankle Int 2017;38:200-7. doi: 10.1177/1071100716666278.
13. Alastuey-López D, Seral B, Pérez MÁ. Biomechanical evaluation of syndesmotic fixation techniques via finite element analysis: Screw vs. suture button. Comput Methods Programs Biomed 2021;208:106272. doi: 10.1016/j.cmpb.2021.106272.
14. Güvercin Y, Abdioğlu AA, Dizdar A, Yaylacı EU, Yaylacı M. Suture button fixation method used in the treatment of syndesmosis injury: A biomechanical analysis of the effect of the placement of the button on the distal tibiofibular joint in the mid-stance phase with finite elements method. Injury 2022;53:2437-45. doi: 10.1016/j.injury.2022.05.037.
15. Williams BT, Ahrberg AB, Goldsmith MT, Campbell KJ, Shirley L, Wijdicks CA, et al. Ankle syndesmosis: A qualitative and quantitative anatomic analysis. Am J Sports Med 2015;43:88-97. doi: 10.1177/0363546514554911.
16. İğde N, Kurt A, Aycan OE, Arslan MC, Bıyıklı T. The impact of proximal fibula resection on foot and ankle biomechanics: A radiological and pedobarographic evaluation. Jt Dis Relat Surg 2025;36:373-82. doi: 10.52312/jdrs.2025.2185.
17. Yaka H, Kesik K, Başbuğ V, Küçükşen MF, Özer M. Is medial or lateral localization of osteochondral lesions of talus related to foot angles? Jt Dis Relat Surg 2024;35:96-104. doi: 10.52312/jdrs.2023.1373.
18. Clanton TO, Campbell KJ, Wilson KJ, Michalski MP, Goldsmith MT, Wijdicks CA, et al. Qualitative and quantitative anatomic investigation of the lateral ankle ligaments for surgical reconstruction procedures. J Bone Joint Surg Am 2014;96:e98. doi: 10.2106/JBJS.M.00798.
19. Demirtas Y, Emet A. The comparison of the two different patella fracture fixation technique: Finite element analysis. IJPTE 2022;2:95-8. doi: 10.56158/jpte.2022.35.1.02.
20. Gray HA, Taddei F, Zavatsky AB, Cristofolini L, Gill HS. Experimental validation of a finite element model of a human cadaveric tibia. J Biomech Eng 2008;130:031016. doi: 10.1115/1.2913335.
21. Sumanont S, Nopamassiri S, Boonrod A, Apiwatanakul P, Boonrod A, Phornphutkul C. Acromioclavicular joint dislocation: A Dog Bone button fixation alone versus Dog Bone button fixation augmented with acromioclavicular repair-a finite element analysis study. Eur J Orthop Surg Traumatol 2018;28:1095-101. doi: 10.1007/s00590-018-2186-y.
22. Beumer A, van Hemert WL, Swierstra BA, Jasper LE, Belkoff SM. A biomechanical evaluation of the tibiofibular and tibiotalar ligaments of the ankle. Foot Ankle Int 2003;24:426-9. doi: 10.1177/107110070302400509.
23. Sikka RS, Fetzer GB, Sugarman E, Wright RW, Fritts H, Boyd JL, et al. Correlating MRI findings with disability in syndesmotic sprains of NFL players. Foot Ankle Int 2012;33:371-8. doi: 10.3113/FAI.2012.0371.
24. Mercan N, Yıldırım A, Dere Y. Biomechanical analysis of tibiofibular syndesmosis injury fixation methods: A Finite element analysis. J Foot Ankle Surg 2023;62:107-14. doi: 10.1053/j.jfas.2022.05.007.
25. Shuler FD, Woods D, Tankersley Z, McDaniel C, Hamm J, Jones J, et al. An anatomical study on the safe placement of orthopedic hardware for syndesmosis fixation. Orthopedics 2017;40:e329-33. doi: 10.3928/01477447-20161219-03.
26. Haraguchi N, Armiger RS, Myerson MS, Campbell JT, Chao EY. Prediction of three-dimensional contact stress and ligament tension in the ankle during stance determined from computational modeling. Foot Ankle Int 2009;30:177-85. doi: 10.3113/FAI-2009-0177.
27. Stauffer RN, Chao EY, Brewster RC. Force and motion analysis of the normal, diseased, and prosthetic ankle joint. Clin Orthop Relat Res 1977;(127):189-96.
28. Soin SP, Knight TA, Dinah AF, Mears SC, Swierstra BA, Belkoff SM. Suture-button versus screw fixation in a syndesmosis rupture model: A biomechanical comparison. Foot Ankle Int 2009;30:346-52. doi: 10.3113/FAI.2009.0346.
29. Forsythe K, Freedman KB, Stover MD, Patwardhan AG. Comparison of a novel FiberWire-button construct versus metallic screw fixation in a syndesmotic injury model. Foot Ankle Int 2008;29:49-54. doi: 10.3113/FAI.2008.0049.
30. Parker AS, Beason DP, Slowik JS, Sabatini JB, Waldrop NE 3rd. Biomechanical comparison of 3 syndesmosis repair techniques with suture button implants. Orthop J Sports Med 2018;6:2325967118804204. doi: 10.1177/2325967118804204.
31. Meekaew P, Paholpak P, Wisanuyotin T, Sirichativapee W, Sirichativapee W, Kosuwon W, et al. Biomechanics comparison between endobutton fixation and syndesmotic screw fixation for syndesmotic injury ankle fracture; A finite element analysis and cadaveric validation study. J Orthop. 2022;34:207-14. doi: 10.1016/j.jor.2022.08.019.

32. Xu HL, Song YJ, Hua YH. Reconstruction of chronic injured distal tibiofibular syndesmosis with autogenous tendon graft: A systematic review. Biomed Res Int 2021;2021:3182745. doi: 10.1155/2021/3182745.
33. Wixted CM, Luo EJ, Stauffer TP, Wu KA, Adams SB, Anastasio AT. Biomechanical profile of varying suture button constructs in cadaveric specimens: A systematic review and meta-analysis. Ann Transl Med 2023;11:344. doi: 10.21037/atm-23-1527.
34. O'Daly AE, Kreulen RT, Thamyongkit S, Pisano A, Luksameearunothai K, Hasenboehler EA, et al. Biomechanical evaluation of a new suture button technique for reduction and stabilization of the distal tibiofibular syndesmosis. Foot Ankle Orthop 2020;5:2473011420969140. doi: 10.1177/2473011420969140.
35. Candal-Couto JJ, Burrow D, Bromage S, Briggs PJ. Instability of the tibio-fibular syndesmosis: Have we been pulling in the wrong direction? Injury 2004;35:814-8. doi: 10.1016/j.injury.2003.10.013.
36. Boyd BS, Doty JF, Kluemper C, Kadakia AR. Anatomic risk to the neurovascular structures with a medially based all-inside syndesmosis suture button technique. J Foot Ankle Surg 2020;59:95-9. doi: 10.1053/j.jfas.2019.07.016.
37. Harper MC, Keller TS. A radiographic evaluation of the tibiofibular syndesmosis. Foot Ankle 1989;10:156-60. doi: 10.1177/107110078901000308.
38. Ostrum RF, De Meo P, Subramanian R. A critical analysis of the anterior-posterior radiographic anatomy of the ankle syndesmosis. Foot Ankle Int 1995;16:128-31. doi: 10.1177/107110079501600304.
39. Elgafy H, Semaan HB, Blessinger B, Wassef A, Ebraheim NA. Computed tomography of normal distal tibiofibular syndesmosis. Skeletal Radiol 2010;39:559-64. doi: 10.1007/s00256-009-0809-4.
40. Chen Y, Qiang M, Zhang K, Li H, Dai H. A reliable radiographic measurement for evaluation of normal distal tibiofibular syndesmosis: A multi-detector computed tomography study in adults. J Foot Ankle Res 2015;8:32. doi: 10.1186/s13047-015-0093-6.
41. Spindler FT, Gaube FP, Böcker W, Polzer H, Baumbach SF. Compensation of dynamic fixation systems in the quality of reduction of distal tibiofibular joint in acute syndesmotic complex injuries: A CT-based analysis. Foot Ankle Int 2022;43:1393-401. doi: 10.1177/10711007221115193.
42. Aitor IG, Galvez-Sirvent E, Martinez-Diez JM, Pallares-Sanmartín J, Kalbakdij-Sanchez C, Mills S, et al. Comparative CT study on syndesmosis mobility after static or dynamic fixation for ankle fractures with syndesmotic rupture: A pilot study. Arch Bone Jt Surg 2022;10:702-11. doi: 10.22038/ABJS.2022.61845.3020.
43. Ramsey PL, Hamilton W. Changes in tibiotalar area of contact caused by lateral talar shift. J Bone Joint Surg Am 1976;58:356-7.
44. Hunt KJ, Goeb Y, Behn AW, Criswell B, Chou L. Ankle joint contact loads and displacement with progressive syndesmotic injury. Foot Ankle Int 2015;36:1095-103. doi: 10.1177/1071100715583456.